Höglind, Mats; Cameron, David; Persson, Tomas; Huang, Xiao; Van Oijen, Marcel. 2020. **BASGRA_N: a model for grassland productivity, quality and greenhouse gas balance.**

The definitive version was published in *Ecological Modelling*, 417, 108925. 13. https://doi.org/10.1016/j.ecolmodel.2019.108925

BASGRA_N: a model for grassland productivity, quality and greenhouse gas balance

Mats Höglind [1,*], *David Cameron* [2], *Tomas Persson* [1], *Xiao Huang* [1], *Marcel van Oijen* [2]

[1] *Norwegian Institute of Bioeconomy Research (NIBIO), 4353 Klepp Stasjon, Norway*

[2] *Centre for Ecology & Hydrology, Bush Estate, Penicuik EH26 0QB, UK*

[*] *mats.hoglind@nibio.no*

2019-11-13

Abstract

The main objective of this paper is to present the new model BASGRA_N, to show how it was parameterized for grass swards in Scandinavia, and to evaluate its performance in predicting above-ground biomass, crude protein, cell wall content and dry matter digestibility. This model was developed to allow simulation of: (1) the impact of N-supply on the plants and their environment, (2) the dynamics of greenhouse gas emissions from grasslands, (3) the dynamics of cell-wall content and digestibility of leaves and stems, which could not be simulated with its predecessor, the BASGRA-model. To calibrate and test the model, we used field experimental data. One dataset included observations of biomass (DM) and crude protein content (CP) under different N fertilizer regimes from five sites in central and southern Sweden. The other dataset included observations DM, and sward components as well as CP, cell wall content (NDF) and DM digestibility as affected by harvesting regime from one site in southwestern Norway. The total number of experiments was nine, of which three were used for model testing. When BASGRA_N was run with the maximum a-posteriori (MAP) parameter vector from the Bayesian calibration for the Swedish test sites, DM and CP were both simulated to an overall Pearson correlation coefficient (R^2) of minimum 0.58, index of agreement (d) of minimum 0.69 and normalized root mean squared error (NRMSE) of maximum 0.30, respectively. Corresponding metrics for Norwegian test sites was were 0.93, 0.96 and 0.27 for DM and >0.73, >0.61, <0.18 for DM digestibility, NDF and CP content. We conclude that

BASGRA_N can be used to simulate yield and CP responses to N with satisfactory precision, while maintaining key features from its predecessor. The results also suggest that DM digestibility and NDF can be simulated satisfactorily, which is supported by results from a recent model comparison study. Further testing of the model is needed for some variables for which we currently do not have enough data, notably leaching and emission of N-containing compounds. Further work will include application of the model to investigate GHG mitigation options, and evaluation against independent data for the conditions for which it will be applied.

1 Introduction

Perennial grasslands occupy between 20 and 40 % of the earth's land surface depending on the definition of vegetation types (Reynolds and Frame, 2005). Grasslands are extremely important for global food supply, providing feed for ruminants. They constitute highly dynamic systems, with frequent foliar losses due to cutting or grazing, and tiller losses due to e.g. adverse weather conditions, and regrowth through remobilization of reserves, tillering and refoliation.

Climate change and rising CO_2 concentration will affect the biomass productivity and stability of grasslands (Ryan et al., 2017; Van Oijen et al., 2018) as well as the quality of their biomass (Dumont et al., 2015). Processe based modelling can be used to study grassland responses to climate change and rising CO_2 levels, and to evaluate adaption and mitigation options including change of management practices and plant breeding efforts.

Process-based grassland models have been developed to identify optimal management practices (Bonesmo and Bélanger, 2002; Graux et al., 2013; Gustavsson et al., 1995; Höglind et al., 2001; Riedo et al., 1998; Rodriguez et al., 1999; Van Oijen et al., 2005; Wu et al., 2007) under current and projected future climate conditions (Persson and Höglind, 2013), and to help evaluate genotypes in plant breeding (Van Oijen and Höglind, 2016). Increasingly, such models simulate not only the quantity of biomass, but also its quality, or more specifically its nutritive value in ruminant feeding (Bonesmo and Bélanger, 2002; Gustavsson et al., 1995; Jégo et al., 2013). All the grassland models mentioned above include sensitivity of the sward to climatic conditions. Some grassland models also include sensitivity to atmospheric CO_2 concentration (Graux et al., 2013; Höglind et al., 2016;

Riedo et al., 1998; Rodriguez et al., 1999).

There are a few grassland models that simulate the biogeochemistry of grassland, i.e. the cycling of carbon (C), nutrients and water through plants, soil and atmosphere such as the PaSim model (Graux et al., 2013; Riedo et al., 1998) and the SPACSYS model which integrate plant growth, carbon (C) and nitrogen (N) cycling and soil water components including a three-dimensional root structure module (Wu et al., 2007) and nitrification and denitrification processes (Wu et al., 2015). Such models are most useful to evaluate climate change impact on soil processes and their interactions with sward nutrient and water use, growth and decomposition. Moreover, to mitigate climate change, grassland management is increasingly expected to not only aim at maximizing productivity and quality, but also at minimizing emissions of greenhouse gases (Kipling et al., 2016). Further model improvement would be useful for an increased understanding of these climate change effects on soil plant C, N and water interactions. There are also dynamic global vegetation models (e.g. LP, ORCHIDEE) and global land surface models (e.g. CLM) which integrate grass growth with biogeochemical processes (C, N and water dynamics). However, in contrast to the grassland models mentioned above, they are less suitable for simulation studies focusing management x environment interactions at field-scale.

Two major complications in modelling productivity, quality and greenhouse gas emissions are the roles of tillering and winter survival. Grassland dynamics is dominated by periods of tillering and tiller death. Tillers form the scaffolding for leaf appearance and, when elongating, constitute major sinks of C and nutrients. However, the extent and nature of tillering and tiller death vary widely among grass species with different life cycles, and growth and development patterns. In addition, tiller dynamics can vary within grass species largely due to climate, weather and management conditions. Under the cold temperate climate conditions and management practices that are typical for Scandinavia and other regions in Northern Europe, tiller death in winter can be high, hampering the growth of the sward next spring (Larsen, 1994). The BASGRA model (Höglind et al., 2016) includes all the processes of tillering, foliar dynamics, winter death and spring regrowth for timothy.These model processes have been developed largely based on empirical knowledge from timothy experiments in Northern Europe, one major production region of this grass species. So far, to our knowledge BASGRA is the only model that simulates tiller dynamics in grasslands.

Recently, processes for the simulation of forage nutritive value and biogeochemical cycling have been incorporated in a new version of the model, from now on called BASGRA_N. These additional modules thus make it possible to simulate the effects of overwintering and tillering on grassland N dynamics. Even though this model version has been applied in two previous studies in the Nordic region of Europe (Korhonen et al., 2018; Persson et al., 2019), no comprehensive description of the BASGRA_N model with its main novel features has been published. Neither did these previous published applications of BASGRA_N include any simulations of the winter period.

The major aim of the paper is to describe the new model BASGRA_N model with processes for the simulation of forage nutritive value and biogeochemical cycling, the Bayesian calibration of its parameters, and to make an evaluation of its performance for variables for which suffiscient data are available for timothy, the Scandinavian region of Northern Europe, a major production region of this species. A second aim is to show examples of model application to timothy grassland in Scandinavia. Climate change impacts on grasslands at these high latitudes is expected to be particularly pronounced (Höglind et al., 2013; Rapacz et al., 2014).

We first present, in Section 2, the new model version BASGRA_N, and describe how it differs from previous versions. Detailed descriptions of are given of features that are unique to BASGRA_N. We then show, in Section 3, how the model was parameterized, and its performance evaluated against observations from field experiments in Sweden and Norway. In Section 4, to illustrate the potential applicability of this model, we show one example application to investigate how key processes underlying biomass accumulation and forage nutritive value respond to N, and another example to assess the scope for optimizing N fertilization, aiming to maximize biomass yield and qualty while minimizing greenhouse gas emissions. The paper is concluded with a discussion of the modelling approach, the need for further evaluation, and an outlook of future applications.

This paper supplements two previous papers in which BASGRA_N was compared with two other grassland models, CATIMO and STICS, with respect to prediction accuracy for biomass quantity and nutritive value (Korhonen et al., 2018; Persson et al., 2019). While observations and simulations were compared for a wide range of conditions in the cited papers, BASGRA_N was only briefly described, and C and N cycling was not studied.

2 Materials and Methods

2.1 The model BASGRA_N

2.1.1 Overview of model versions

BASGRA_N is a new version of the BASGRA model, which was developed to allow for daily simulation of (1) the impact of N-supply on the plants and their environment, (2) the dynamics of greenhouse gases in plants and soil, (3) the dynamics of cell-wall content and digestibility of leaves and stems.

A description of the predecessor of BASGRA, named BASGRA_2014, includes variables for carbon in above- and below-ground plant parts, plant phenology including elongation, tillering, vernalization, frost kill and overwintering, and soil water and carbon and snow depth (Höglind et al., 2013). Plant biomass is simulated with a daily time step as a function of radiation, temperature, precipitation, wind speed, humidity, atmospheric CO2 concentration and a calendar indicating the days when the sward is cut. The code of BASGRA_2014 and a detailed user guide can be downloaded from http://dx.doi.org/10.5281/zenodo.27867.

We now turn to the new parts of the model, i.e. what distinguishes BASGRA_N from BASGRA_2014. BASGRA_N, a user guide and technical details of the model implementation can be downloaded from https://doi.org/10.5281/zenodo.1493404. BASGRA_N includes a novel algorithm for the dynamics of foliar N. The dynamics of cell-wall content and digestibility are simulated using simple empirical functions of phenological stageas described below.

A comprehensive list of abbreviations used in this paper is provide in Table 1. A flowchart for C and N, which illustrates the general framework of coupled C/N biogeochemical processes in BASGRA_N, is provided in Fig. 1

Table 1: Explanation of variable abbreviations.

Variable	Description	Units
CRES	C pool of grass reserves	g C m^{-2}

Variable	Description	Units
CLV	C pool of grass leave	g C m^{-2}
CST	C pool of grass stem	g C m^{-2}
CSTUB	C pool of grass stub	g C m^{-2}
CRT	C pool of grass root	g C m^{-2}
CSOMF	C pool of grass fast-decomposing SOM	g C m^{-2}
CSOMS	C pool of grass slow-decomposing SOM	g C m^{-2}
NSH	N pool of grass shoot	g N m^{-2}
NSTUB	N pool of grass stub	g N m^{-2}
NRT	N pool of grass root	g N m^{-2}
NMIN	N pool of soil mineral N	g N m^{-2}
NSOMF	N pool of grass fast-decomposing SOM	g N m^{-2}
NSOMS	N pool of grass slow-decomposing SOM	g N m^{-2}
LAI	Leaf Area Index	m^2 m^{-2}
LT50	Lethal temperature at which 50% of tillers die due to frost injury	Â°C
NCSHMAX	Maximum N-C ratio of shoot	g N g^{-1} C
K	Light extinction coefficient	m^2 m^{-2}
RUBISC	Rubisco-content	g m^{-2}
KN	Extinction coefficient for N	m^2 m^{-2}
KNMAX	Maximum value of nitrogen extinction coefficient	m^2 m^{-2}
DLAI	Death of leaf area	m^2 m^{-2}
DNSH	N loss of shoot	g N m^{-2}
DLV	C loss of leaf	g C m^{-2}
TILV	Vegetative tillers	tillers m^{-2}
TILG1	Generative non-elongating tillers	tillers m^{-2}
TILG2	Generative elongating tillers	tillers m^{-2}
RLEAF	Leaf appearance rate per tiller	leaves $tiller^{-1}$ m^{-2}
PHEN	Phenological stage	-
DM	Shoot biomass	g DM m^{-2}

Variable	Description	Units
F_PROTEIN	Crude protein	g g^{-1} DM
F_DIGEST_DM	DM digestibility	g g^{-1} DM
F_WALL_DM	Neutral detergent fibres (cell walls)	g g^{-1} DM
F_ASH	Ash	g g^{-1} DM
LERG	Leaf elongation	mm d^{-1}
NELLVG	Elongating leaves	$tiller^{-1}$
RES	Water soluble carbohydrates	g g^{-1} DM
SLA	Specific leaf area	m^2 g^{-1}
TILTOT	Tiller density	m^{-2}

2.1.2 New state variables and processes for biogeochemical cycling, inputs, outputs and parameters

BASGRA_N has one more plant state variable than BASGRA_2014: the amount of N in above-ground plant parts (NSH; g N m^{-2}). N in roots is simulated as root C times a constant N-C ratio, and N in reserves is considered absent. The model has seven extra environmental state variables representing mineral N, and both C and N in three other soil pools: litter and two forms of organic matter differing in decomposition rate. This brings the total number of state variables in BASGRA_N to 31 (14 plant, 17 environment).

The dynamics of NSH are the net result of growth (incorporating N taken up from the soil and from remobilisation), senescence and harvesting. The dynamics of the seven state variables for C and N in the soil are simulated in the same way as in the forest model BASFOR (Van Oijen et al., 2005). The pool sizes vary as a result of external inputs (fertilisation, deposition), decomposition, uptake by plants, and losses to the environment (leaching, gaseous emissions).

BASGRA_N requires the same input variables as BASGRA_2014, plus new input time series for N fertilisation and for atmospheric N deposition, both expressed in g N m^{-2} d^{-1}. In the archived version of BASGRA_N, 31 state variables as well as process rates and intermediate variables of

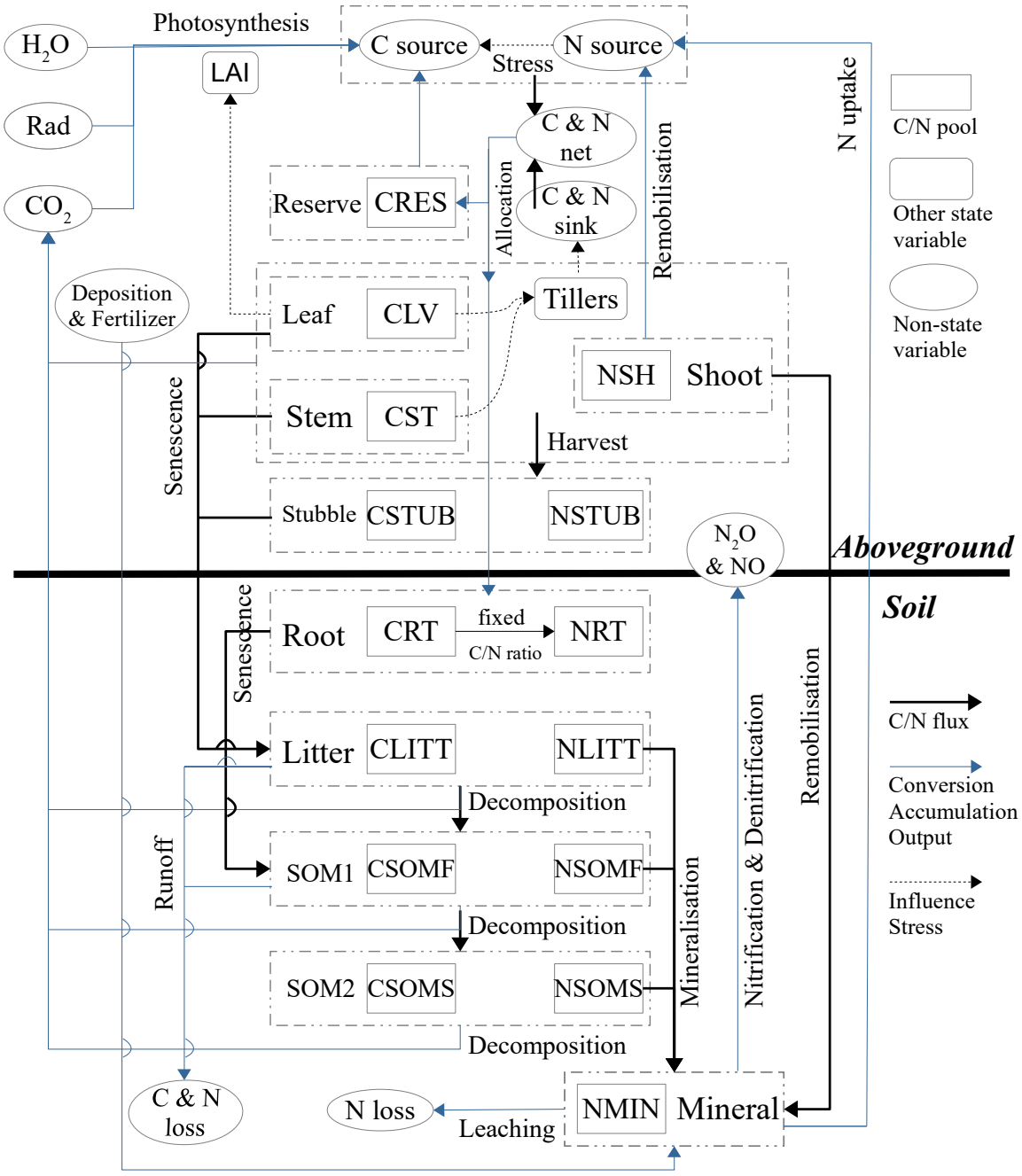

Figure 1: The Framework of BASGRA_N for C-N Biogeochemical Modelling

the C, N and water cycles, and of cell-wall content and digestibility are specified by default. New outputs also include crude protein content and ash content, which are estimated as linear functions of shoot N content. In total there are 113 parameters in BASGRA_N including initial constants for N in above-ground plant parts, control coefficients for new processes, N-C ratios and relative death rates of roots and stubble.

2.1.3 N-profile and remobilisation

At every time step, the availability of N to the plants is determined by the amount of soil mineral N (state variable NMIN; g N m^{-2}), plus the amount of N that becomes available from within the shoots by remobilisation. N-remobilisation is calculated by comparing the actual amount of N present in the shoots (NSH) to the amount of N that would have been present if N-C ratio followed the same exponential profile in the sward as light, starting from the maximum N-C value allowed by the model at the top (NCSHMAX). Similarities and differences between the vertical profiles of light and N have been investigated theoretically and empirically before (Charles-Edwards, 1982; Dreccer et al., 2000; Hikosaka, 2016; Van Oijen et al., 2004) and form the basis of the approach described here. In the model, the amount of shoot N is called NSHK, i.e. "the amount of N in shoots if the N profile would follow the light extinction coefficient K". There will generally be more N in the sward than NSHK because the N profile of vegetation tends to be more uniform than the light profile (Dreccer et al., 2000; Hikosaka, 2016), as depicted in Fig.2.

The formula for NSHK is the following:

$$NSHK = CSH * NCSHMAX * \frac{1 - exp(-K * LAI)}{K * LAI},$$

where CSH is shoot C, i.e. C in leaves plus stems. The term "$CSH * NCSHMAX$" is the maximum possible amount of shoot-N (maximum N-C ratio at all positions), and the final term is the fraction of that maximum that is realised in an exponential profile with coefficient K. When NSH becomes greater than NSHK, the excess N (NSH - NSHK) becomes available for growth at a given time constant, representing the process of N remobilisation.

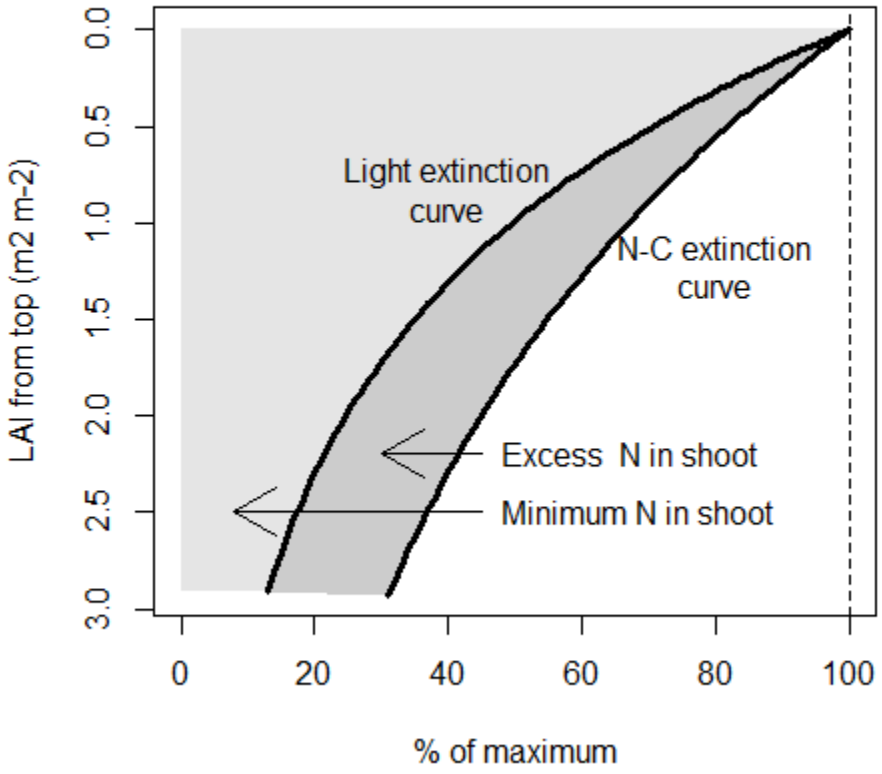

Figure 2: Exponential vertical profiles of light and nitrogen in the foliage in BASGRA_N. The extinction coefficient for light (K) is typically larger than for nitrogen (N). Nitrogen in excess of the light-extinction profile can be remobilised. Growth and harvesting operate at the top of the canopy and senescence at the bottom, so the latter process has least impact on shoot nitrogen content

2.1.4 Sink strength for N

In all versions of BASGRA, allocation of C to shoot growth depends on the balance between C-availability (from photosynthesis and reserves) and C-demand by leaves and stems. We refer to the shoot demand for C as its "sink strength". In BASGRA_N, a small N-source reduces shoot sink strength, but does not affect the sink strength of other processes. The effect of a limiting N-source on the shoot sink (for growth in terms of C) is assumed to be proportional to the N-source divided by the product of shoot sink and a maximum shoot N-C ratio. The latter product can be viewed as the N-sink of the plants. So shoot C sink is proportional to the source-sink ratio for N. In yet other words, when the N-source is too low to support shoot growth at maximum N concentration, shoot growth rate is reduced proportionately. The proportionality factor is called 'fNgrowth'.

2.1.5 Effects of N-limitation on other plant processes than growth

Apart from influencing shoot sink strength and thereby allocation patterns, N-limitation does not have an immediate effect on plant light-use efficiency because the Rubisco-content and N-C ratio of upper leaves (parameter RUBISC, g m^{-2} leaf; parameter NCSHMAX, g g^{-1}) are assumed to be constant. However, the leaf appearance rate, which provides sites for tillering, is proportional to fNgrowth. Note also that all plant processes will, directly or indirectly, be affected in the long-run by any changes in C and N allocation between plant parts.

2.1.6 Dynamics of plant N-C ratios

The overall N-C ratio of stems and leaves, NCSH, does not fluctuate strongly despite being affected by growth, senescence and harvesting. All three processes change NCSH by adding or removing tissue that is not at the average N-C ratio. We assume that (1) growth adds young material at a ratio higher than average, (2) harvesting removes tissue also at higher-than-average N-C ratio, while (3) senescence removes tissue at lower than average N-C ratio.

Calculation of the N-C ratios at which the three processes proceed is based on the assumption that N concentration follows an exponential function of LAI, counting from the youngest leaves

downward. So when the shoot biomass is small and thus also the LAI, the N-C ratio of the plant is close to the maximum N-C ratio (parameter NCSHMAX). As the LAI increases, the N-C ratio decreases. Likewise, the harvested material from a very small cut when LAI is small would have high N-C ratio whereas cuts at large LAI would have lower N-C ratio. The loss of N in senescence also adheres to the concept of an exponential aboveground profile of N, but the assumption here is that the lowest-N tissue dies first, so days with high senescence may have only slightly greater losses of N per unit tissue than days with only minor senescence. All these calculations require us to estimate KN, the "extinction coefficient for N" in the sward profile.

2.1.7 Derivation of the N-extinction coefficient, KN

Assuming that the N-C ratio follows an exponentially decreasing curve in the canopy, starting from a given maximum N-C ratio at the top (NCSHMAX), we should in principle be able to calculate the N extinction coefficient (KN) as a function of total aboveground leaf area (LAI) and total aboveground N (NSH). However, as we show now, there is no analytical solution to this problem, so we developed a new approximate equation for KN.

As a general observation, we can say that if NSH > NSHK, then KN must be less than K (N "extinguishes" less quickly than light does) and vice versa. More precisely, KN can be solved from the following equation, similar to the one for NSHK above but with a different exponential coefficient:

$$NSH = CSH * NCSHMAX * \frac{1 - exp(-KN * LAI)}{KN * LAI}.$$

Unfortunately that equation cannot be solved analytically for KN, because of the exponential term. However, we can find an approximation to KN by replacing the exponential term by its third-order Taylor expansion around KN equal to zero. Plugging that approximation into the equation for NSH gives a quadratic equation that can be solved:

$$NSH \approx CSH * NCSHMAX * (1 - \frac{KN * LAI}{2} + \frac{KN^2 * LAI^2}{6}),$$

and the solution of this quadratic equation is:

$$KN \approx \frac{3/2 \pm \sqrt{6\,NSH/(CSH * NCSHMAX) - 15/4}}{LAI}.$$

So this equation gives an appromixation for the coeffient with which N concentration decreases exponentially from the top to the bottom of the canopy. The approximation can be used for any vegetation with an exponential profile of N. Note that $NSH/(CSH * NCSHMAX)$ must be larger than 5/8 to ensure that the square root is real. The approximation will become poor for large LAI, but we can derive an upper bound for KN from the original equation for NSH as follows. Because the term (1 - exp(KN*LAI)) < 1, we find that:

$$KN < KNMAX = \frac{CSH * NCSHMAX}{NSH * LAI}.$$

We now check the quality of the approximation for KN for two extreme values of NSH: $NSH = CSH * NCSHMAX$ and $NSH = NSHK$. We begin with the first case where we have a uniform profile of N with an N-C ratio that is everywhere equal to NCSHMAX. In other words, KN should be zero. We check this by plugging $NSH = CSH * NCSHMAX$ into our approximative equation for KN and find that it simplifies to:

$$\text{NSH uniform} \implies KN \approx \frac{3/2 \pm \sqrt{6 - 15/4}}{LAI} = \frac{3/2 \pm 3/2}{LAI},$$

and this indeed simplifies to $KN = 0$ provided we choose the "minus"-solution of the quadratic equation. We now turn to the second case: $NSH = NSHK$. In that case we should find - if our approximative equation applies - that KN is about equal to the light extinction coefficient K. So we plug the equation given above for NSHK into our approximative equation for KN and find:

$$\text{NSH=NSHK} \implies KN \approx \frac{3/2 \pm \sqrt{6\,\frac{1-exp(-K*LAI)}{K*LAI} - 15/4}}{LAI}.$$

We checked this result numerically for a broad range of values of K and LAI. For small values

of $K * LAI$, the approximation is excellent, i.e. $KN \approx K$. For large values of $K * LAI$, the approximation is an overestimate, but the upper bound for KN that we found ($KNMAX = CSH * NCSHMAX/(NSH * LAI)$) then comes to the rescue: KNMAX becomes increasingly close to the light extinction coefficient K, so the overestimation is constrained. We can see that as follows:

$$\text{NSH=NSHK} \implies KNMAX = \frac{CSH * NCSHMAX}{NSHK * LAI} = \frac{K}{1 - exp(-K * LAI)},$$

where the denominator of the final ratio gets increasingly close to unity when $K * LAI$ becomes big. So also for this very different case, the approximative equation for KN, with upper bound, works well. Taking everything together, we work with the following rule for KN in the model:

If $NSH/(CSH * NCSHMAX) \geq 5/8$ then KN is assumed equal to the minus-solution of the approximative quadratic equation or to KNMAX, whichever is smaller,

If $NSH/(CSH * NCSHMAX) < 5/8$ then KN is assumed equal to KNMAX.

2.1.8 KN: rule and role

The role of KN in the model is to ensure that the effects of growth, harvesting and senescence on NSH are calculated correctly. These processes increase or decrease shoot biomass. The amount of N that is gained or lost should be consistent with the N-profile as measured by KN. Here below, we only show how this is calculated for senescence, but similar equations apply to the two other processes. Daily senescence removes an amount DLAI from the LAI. The fraction of C lost is less than DLAI/LAI because we assume that stems do not senesce. And the fraction of N lost in the same process is even less because we assume that senescent tissue is at the lower end of the exponential profile of N-C ratio in the canopy. We calculate the fraction of NSH lost in senescence as 1 minus the fraction of N remaining in leaves (stems are disregarded), and for that calculation we use the concept of the N extinction coefficient, i.e. KN. The fraction of leaf biomass remaining (i.e. not senescing) is $(LAI - DLAI)/LAI$. The fraction of leaf N in the corresponding part of the exponential curve is equal to:

$$\text{Fraction non-senescing leaf N} = \frac{1 - exp(-KN * (LAI - DLAI))}{1 - exp(-KN * LAI)}.$$

So our estimate for the fraction of leaf N lost in daily senescence is 1 minus that amount. We may need to correct that estimate because KN is only approximated and not exactly known. We ensure that the N-C ratio of the senescing leaf tissue is not so low that the remaining biomass has more than the maximum permitted N-C ratio, NCSHMAX:

$$DNSH \geq NSH - NCSHMAX * (CSH - DLV),$$

where DLV is the C loss from dying leaves in senescence. So, we take the loss of shoot N in senescence, DNSH, to be the maximum of our profile-based estimate and the amount needed to ensure that $NCSH \leq NCSHMAX$.

2.1.9 Simulation of N in the soil

The simulation of C and N in the soil follows the scheme for C devised by Goudriaan (1990), which we extended with N dynamics (Van Oijen et al., 2005). We distinguish three organic pools in the soil: litter ("LITT"), organic matter with a fast turn-over rate ("SOMF"), and organic matter with a slow turn-over rate ("SOMS"). Each pool contains both C and N, and their ratios can vary to some extent. So there are six state variables CLITT, CSOMF, CSOMS, NLITT, NSOMF, and NSOMS. Shoot senescence contributes to LITT, at the N-C ratio of the senescing material, and root senescence contributes to SOMF at the N-C ratio of the roots. Furthermore there are continuously operating transformations from LITT to SOMF to SOMS, in each case with some of the C being lost as CO_2 and some of the N being lost to the soil mineral pool NMIN.

The maximum plant uptake rate of soil mineral N is calculated as NMIN divided by a given time constant. Apart from plant uptake, NMIN is also depleted by loss to the environment (leaching to ground water, emission to the atmosphere), and it is replenished from decomposition of organic material and from external inputs in the form of deposition and fertilisation. This makes NMIN into a highly dynamic variable that never contains more than a small fraction of total soil N, but

one that plays a key role in regulating plant processes. So, the N-source available for growth is equal to the excess of shoot-N plus soil mineral N, both terms divided by their own time constant.

2.1.10 Simulation of cell-wall content and digestibility

Our submodel for cell-wall content and digestibility is intermediate in complexity between the les complex model of Gustavsson et al. (1995) and the more complex of Bonesmo & BÃ©langer (2002). BASGRA_N simulates the dynamics of cell-wall content (g g^{-1} DM) and digestibility (dimensionless) of leaves and stems. Cell-wall content (F_WALL_DM) is calculated separately for leaves, stems and stubble. All dry matter other than cell walls is assumed to be 100% digestible. Digestibility of cell walls (F_DIGEST_DM) decreases linearly with the phenological state of the sward (Nordheim-Viken and Volden, 2009). Leaves, stems and stubble have different cell wall fractions but cell-wall digestibility itself does not differ between the different plant components. The cell-wall contents of both leaves and stems increase linearly with phenological state and are generally higher in stems than in leaves (Nordheim-Viken and Volden, 2009). Cell-wall content of reserves is zero and of stubble 100%.

BASGRA_N distinguishes three types of tillers: vegetative tillers (TILV), generative non-elongating tillers (TILG1) and generative elongating tillers (TILG2), all in units of tillers per m^2. The process of tillering consists of the formation of new vegetative tillers which can progress to the other stages: TILV -> TILG1 -> TILG2. The formation of new tillers is tightly coupled with the process of leaf appearance (RLEAF; number of leaves per tiller per day) on vegetative tillers because new tillers are formed in leaf axils and leaves are formed on tillers. Not all leaf axils are occupied by tillers: site filling is reduced when LAI is high or reserves are low. Leaf appearance is temperature dependent, with a constant phyllochron, but it slows down under drought, N-limitation, short day lengths, and when the sward becomes dominated by elongating tillers at an advanced phenological stage (PHEN; dimensionless). PHEN is reset to zero after every cut and then increases at a rate which is highest at high temperature and long day lengths. The rate at which vegetative tillers move to the first generative category has a temperature optimum and is reduced at short day lengths. Generative tillers move from the non-elongating to the elongating category at a constant relative rate as long as day lengths are long enough. For vernalization-dependent genotypes, generative tillers only form

if the vernalization requirement (temperature dropping below a threshold) has been fulfilled.

The three categories of tillers differ in various respects. Only the elongating tillers acquire significant stem weight, and when the sward is harvested, only non-elongating tillers survive because their apex is below cutting height. Apart from the effect of N-limitation, all the above mechanisms are implemented in the same way as for BASGRA_2014, and for more details we refer to the documentation for that model (Höglind et al., 2016).

The nutritive value of the sward depends to a large extent on fibre content, which is proportional to the fraction of biomass that is in cell walls. Cell wall content is assumed to increase linearly with phenological stage (PHEN), using different functions for leaves and stems, with higher coefficient values for the latter. Because PHEN is reset to zero after each cut, cell wall content is then minimal and increases between cuts.

Another key measure of feed quality, i.e. crude protein (CP) content (g m^{-2}), is modelled as 6.25 times the N content of the sward, using the standard conversion factor.

2.2 Data

Two datasets consisting of observations from field experiments were used to calibrate and evaluate the performance of the model by comparing simulations and observations.

The first dataset consisted of observations of mixed swards of timothy (*Phleum pretense* L; cv. Vanadis; seeding rate 12 kg ha^{-1}) and meadow fescue (*Festuca pratensis* L; cv. Svalöf Sena; seeding rate 8 kg ha^{-1}) carried out on five locations in Sweden, with one or two fields per location and a total of seven fields (Table 2). The fields were established either in 1984 with measurements taken in 1985-1986, or established in 1986 with measurements in 1987-1988. Three N levels were compared. One treatment received no N fertilizer (N0), whereas the others were fertilized with 140 (N1) and 200 kg N ha^{-1} $year^{-1}$ (N2), respectively, split into one application (57-60% of the total N applied) in early spring and one application after the first cut. Shoot biomass (g DM m^{-2}) and its CP content were determined with sampling intervals of 7-14 days from approx. 2 to 16 June during primary growth, and from approx. 14 July to 8. September during secondary growth. In all experiments, P and K were applied according to local recommendations, taking into account soil nutrient status and

expected yield. Weather data were collected from network stations of the Swedish Meteorological and Hydrological Institute (SMHI) near the experimental locations. For details, see Eckersten et al. (2007) and references therein.

The second dataset consisted of observations of the timothy cv. Grindstad from experiments carried out at the location Særheim in Norway (Table 2). There were two experiments. The first was established in 1999, with measurements taken in 2000. The other experiment was established in 2000, with measurements taken in 2001 and 2002. Two cutting regimes were compared in each field (early or late primary cut followed by regrowth and secondary cut), under a common N fertilizer regime aimed to allow for N-unlimited growth. These fields were fertilized with 220 kg N ha^{-1} $year^{-1}$ split into one spring application (140 kg N ha^{-1}) and one application after the first cut (80 kg N ha^{-2}). From April to August each year, with sampling intervals of 7-14 days, shoot biomass (g DM m^{-2}), LAI, specific leaf area (SLA), tiller density, leaf appearance rate, number of elongating leaves per tiller, leaf elongation rate per actively growing leaf were determined, and the shoot biomass was analysed for water soluble carbohydrates ("reserves""; RES), neutral detergent soluble fibres (NDF or"cell walls""; F_WALL_DM), CP, and DM digestibility (F_DIGEST_DM). P and K were applied in spring at 30 and 150 kg ha^{-1}, respectively. Weather conditions were registered at an on-site weather station within 200 m from the fields. For details, see Höglind et al. (2005).

For sites with two experiments, one of them was used for calibration and the other for testing. This gave us five fields for calibration and two for model testing from Sweden, and two for calibration and one for testing from Norway, each with two years of observation except for Særheim (Table 2).

Table 2: Sites with field experiments from which data was collected for calibration and testing of the BASGRA_N model.

Location	Latitude	Longitude	Soil_type	Calibration	Validation
Karlslund	59.47 N	17.75 E	Clay loam	1987-1988	
Klevarp	57.74 N	14.30 E	Sandy loam	1985-1986	1987-1988
Kungsängen	59.84 N	17.65 E	Clay	1985-1986	1987-1988
Lanna	58.35 N	13.13 E	Clay loam	1985-1986	

Location	Latitude	Longitude	Soil_type	Calibration	Validation
Tönnersa	56.57 N	12.98 E	Loamy sand	1987-1988	
Særheim	58.76 N	5.65 E	Sandy loam	2000-2001	2002

2.3 Calibration and testing

We carried out two separate calibrations and tests of the calibrated model, one using the Swedish dataset and one using the Norwegian one. The Swedish dataset allowed us to compare simulated and observed biomass and CP content under different N fertilizer regimes and a common harvesting regime. The Norwegian dataset allowed us to compare simulated and observed values for a larger number of plant variables as affected by harvesting regime, but under a common N fertilizer regime. This dataset was used to calibrate the previous model BASGRA 2014 (Höglind et al., 2016), allowing for indirect comparison of BASGRA-N with its predecessor against a common dataset.

The calibration method was Bayesian, by means of Markov chain Monte Carlo (MCMC) using the Metropolis algorithm (Metropolis et al., 1953; Van Oijen et al., 2005). The same method was previously used to calibrate BASGRA 2014 (Höglind et al., 2016). Prior parameter ranges for new individual parameters in BASGRA_N were derived from literature studies (Höglind et al., 2001; Van Oijen et al., 2005) where available, whereas wide ranges of plausible values were assumed otherwise. All plant parameters were treated as site-independent, whereas soil parameters were considered site-specific. In total, 61 parameters were included in the calibration. Chain length in the MCMC was 1,000,000 for the Swedish dataset, and 300,000 for the Norwegian dataset to ensure convergence for all parameters. For more details on the calibration method and its application to BASGRA, see Van Oijen et al. (2005) and Van Oijen and Höglind (2016).

To quantify the performance of model simulation, we used the Pearson correlation coefficient (R^2), Normalized Root Mean Square Error (NRMSE) and Willmott's index of agreement (d) to test the linear correlation, mismatch and agreement, repectively, between observations and simulations. The value of R^2 greater than 0.5 generally indicates a strong positive correction of the two variables. The value of NRMSE approaching 0 and the value of d approaching 1 indicates the perfect skill of

numerical model to match the measurements. The calculations for the 3 metrics are as followed:

$$R^2 = \frac{cov(\mathbf{X}, \mathbf{Y})}{\sigma_{\mathbf{X}}\sigma_{\mathbf{Y}}}$$

$$NRMSE = \frac{\sqrt{\frac{1}{N}\sum_{i=1}^{N}(x_i - y_i)^2}}{E(\mathbf{Y})}$$

$$d = 1 - \frac{\sum_{i=1}^{N}(x_i - y_i)^2}{\sum_{i=1}^{N}(|x_i - E(\mathbf{Y})| + |y_i - E(\mathbf{Y})|)^2}$$

where, $\mathbf{X}$ and $\mathbf{Y}$ are the time series of model simulations and observations; x_i and y_i are the ith values of the series; N is the length of the series for calibration and validation.

2.4 Application

To highlight the applicability of the model, we show an example in which the model was used to study the effect of N fertilization on the quantity and quality of biomass, and its impact on the environment including greenhouse gas emissions and N budgets for one of the test sites. We also use BASGRA_N to assess the scope for optimizing N fertilization at this site. Even though there were no observed data to compare the simulation outputs from the applications with, hence meaning that these outputs were uncertain, the examples illustrate how this model can be used to complement experimental research.

3 Results

3.1 Calibration and testing

The Bayesian calibration was carried out using data from six sites on a total of 13 variables, in two separate datasets. Tables 3 and 4 give an overview of the behaviour of BASGRA_N when run with the MAP (maximum a-posteriori) parameter estimates from the Bayesian calibration for the Swedish sites. Using this parameter vector, DM and CP were simulated to an overall NRMSE of maximum 0.3, with slightly lower values for the calibration dataset compared with the test datasets (Table 3 and 4, respectively). A corresponding overview of the behaviour of BASGRA when run with the MAP for the Norwegian site is provided in Table 5 and 6. For this site, nearly all variables were

simulated to an overall NRMSE less than 0.5 for the calibration dataset, whereas for the test dataset 2/3 of the variables were simulated with corresponding precision (Table 5 and 6, respectively). The best fit between simulations and observations were observed for DM digestibility, NDF and CP content, with overall NRMSE values below 0.2 for both calibration and test dataset.

The impact of the Bayesian calibration on the behaviour of the model with respect to simulated time courses for all calibration and test sites in Sweden are shown in Supplementary data, Fig. S2. The temporal dynamics of the two variables DM and CP were in general well captured, with a tendency of N-fertilized swards being better captured than non-N fertilized swards. Corresponding time courses for both harvest regimes at the calibration and test site Særheim in Norway, where 13 variables were studied under a common N regime, are shown in Supplementary data, Fig. S3. The temporal dynamics at this site were well captured in general although in some aspects more satisfactorily for DM and CP content than for DM digestibility and NDF content. The later tended to be overestimated although their temporal dynamics were well captured.

Table 3: Model performance for the Swedish calibration dataset. Obs.= mean of observations, Sim. = mean of simulations.

Variable	n	Obs.	Sim.	R^2	d	NRMSE
DM	237	317.77	297.53	0.93	0.96	0.27
F_PROTEIN	234	0.12	0.11	0.75	0.83	0.22

Table 4: Model performance for the Swedish test dataset. Obs.= mean of observations, Sim. = mean of simulations.

Variable	n	Obs.	Sim.	R^2	d	NRMSE
DM	93	273.46	246.20	0.91	0.94	0.29
F_PROTEIN	93	0.13	0.13	0.58	0.69	0.30

Table 5: Model performance for the Norwegian calibration dataset. Obs.= mean of observations, Sim. = mean of simulations.

Variable	n	Obs.	Sim.	R^2	d	NRMSE
DM	49	418.35	401.21	0.98	0.98	0.19
F_PROTEIN	44	0.17	0.16	0.95	0.94	0.18
F_DIGEST_DM	44	0.76	0.81	0.71	0.70	0.09
F_WALL_DM	44	0.54	0.61	0.76	0.66	0.14
F_ASH	44	0.07	0.09	0.65	0.53	0.39
LAI	45	4.00	3.72	0.80	0.88	0.31
LERG	54	0.01	0.01	0.33	0.59	0.48
NELLVG	54	1.63	1.20	0.57	0.67	0.59
RES	45	0.13	0.10	0.52	0.55	0.40
RLEAF	52	0.13	0.09	0.56	0.67	0.48
SLA	45	0.03	0.02	0.44	0.51	0.27
TILTOT	62	2941.44	2905.75	0.71	0.77	0.24

Table 6: Model performance for the Norwegian test dataset. Obs.= mean of observations, Sim. = mean of simulations.

Variable	n	Obs.	Sim.	R^2	d	NRMSE
DM	31	329.82	327.31	0.93	0.96	0.27
F_PROTEIN	27	0.17	0.16	0.91	0.92	0.18
F_DIGEST_DM	27	0.72	0.79	0.73	0.66	0.11
F_WALL_DM	27	0.55	0.63	0.85	0.62	0.15
F_ASH	27	0.06	0.09	0.42	0.46	0.47
LAI	30	3.58	2.78	0.54	0.62	0.66
LERG	26	0.01	0.01	0.16	0.50	0.60

Variable	n	Obs.	Sim.	R^2	d	NRMSE
NELLVG	27	1.63	0.99	0.75	0.73	0.52
RES	27	0.13	0.10	0.13	0.40	0.42
RLEAF	27	0.14	0.07	0.51	0.57	0.66
SLA	30	0.03	0.02	0.62	0.67	0.24
TILTOT	30	2369.37	2576.01	0.49	0.65	0.30

3.2 Application

3.2.1 Effects of N-fertilization on quantity and quality of biomass

We now show an example of application of BASGRA_N for the simulation of two years of growth of timothy at Kungsängen from the experiment with three levels of N-fertilization carried out in 1987-1988. The aim is to illustrate how simulations with BASGRA_N can be used to study interactions between weather and N fertilization management on the dynamics of leaves and tillers, the allocation of biomass to leaf and stem fractions, and ultimately the nutritive value of the biomass in terms of protein and cell wall concentrations and cell wall digestibility.

Fig. 3 shows time series of overall tiller density. The simulations shows large drops in tiller density at harvest times. After cutting, tiller densities initially increase again, but then start to drop in the case of the treatments with applied N fertilizers. This pattern is repeated in both growing seasons, and tiller formation ceases during the intervening winter months. We examine the causes of this complex behaviour below.

For clarity of presentation, we focus on the first growing season in the next few plots. Absolute and relative tiller densities, in each of the three categories, are shown in Fig. 4. The figure shows major differences between the fertilization-treatments in the density of vegetative tillers. At low N, vegetative tillers slowly increase their density after cutting, reaching a plateau after about a month. In the other two treatments, vegetative tillers increase much faster after cutting but already after two weeks their densities start to decrease, losing over half the tillers in about six weeks. Some of this vegetative tiller loss is due to tillers becoming generative, but given the loss in total tiller

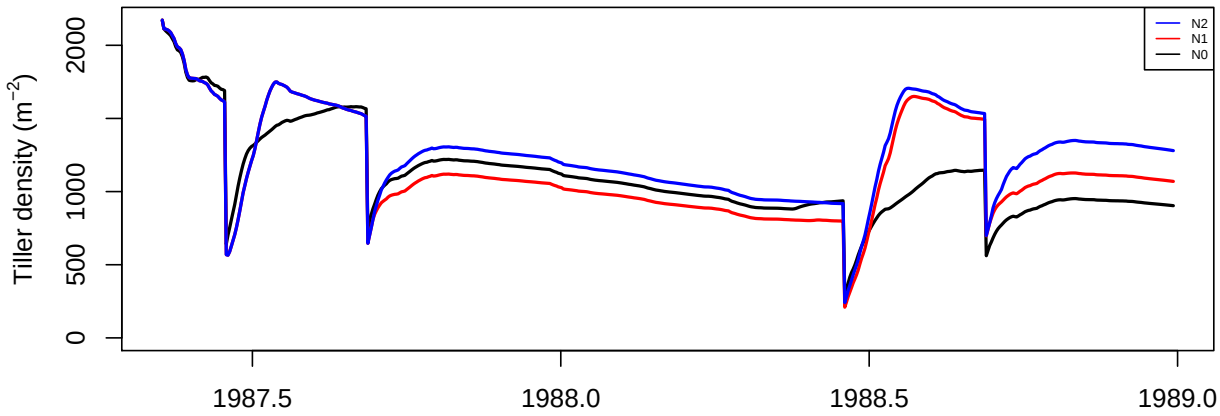

Figure 3: Simulated total tiller density at Kungsängen in 1987-1988 for N application rates 0 (NO), 140 (N1), and 200 (N2) kg N ha^{-1} year^{-1}

density (Fig. 3), some of the losses at high N must be the result of tiller death. We next analyse the causes of these differences between fertilization levels in birth and death of tillers (Fig. 5).

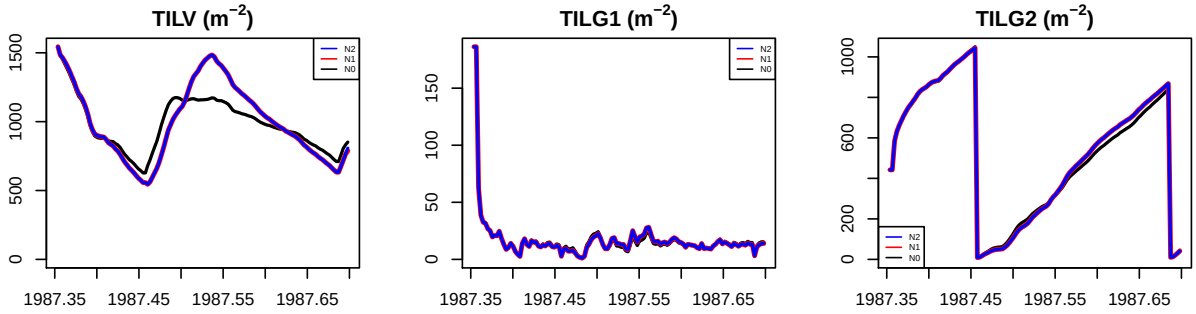

Figure 4: Simulated density of vegetative (TILV), non-elongating (TILG1) and elongating generative tillers (TILG2) at Kungsängen in 1987 for N application rates 0 (NO), 140 (N1), and 200 (N2) kg N ha^{-1} year^{-1}

The top row of Fig. 5 shows the main internal driver of vegetative tiller formation, i.e. leaf appearance, as well as the relative rate at which new tillers are formed on existing ones. Here we see a consistent pattern of higher leaf appearance rate at higher N supply (top left panel) leading to higher rates of tiller formation per vegetative tiller per day (top right panel). The explanation for ultimately higher tiller densities at high N supply is thus tied more to differential rates of tiller appearance than to differential rates of tiller death, although tiller loss is somewhat larger at higher N supply (not shown). After cutting, LAI recovers much better at high N than at low N (bottom left panel). This leads to a lower stem: leaf ratio in the biomass at high N (bottom right panel),

subsequently affecting its chemical composition.

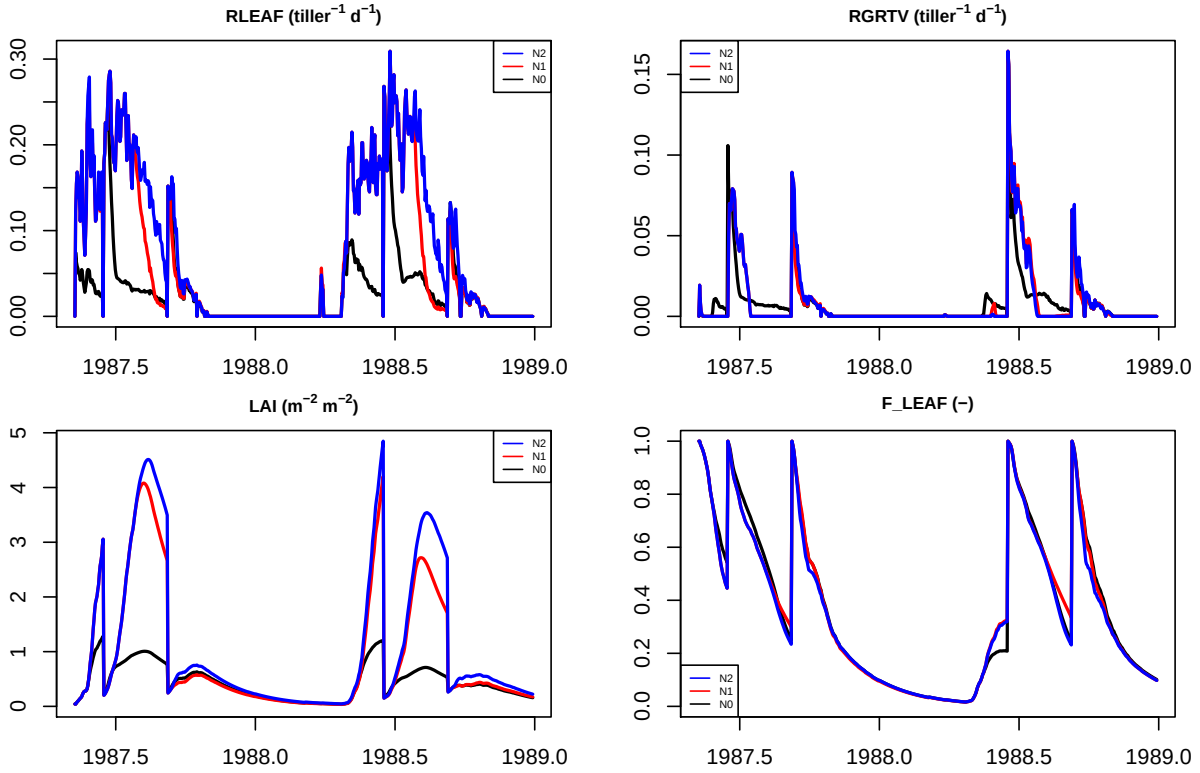

Figure 5: Simulted rate of leaf appearance (RLEAF), rate of tiller appearance (RGRTV), leaf area index (LAI) and proportion of leaves in shoot biomass (F_LEAF) at Kungsängen in 1987-1988 for N application rates 0 (NO), 140 (N1), and 200 (N2) kg N ha^{-1} year^{-1}

The concentration of crude protein and cell walls in the shoot DM are shown in Fig. 6. Protein content responds strongly to N supply. This strong response is due to the combined effect of increased overall content of N in plant tissues, and increased proportion of leaves in biomass, with a higher N concentration than stems, with increasing N supply. The figure also show that concentrations cell walls in biomass responds to some extent to N supply. The lower cell wall content at high N is linked to the higher leaf:stem ratio (Fig. 5) and the slower rate of decline in cell wall content in leaves compared with stems. Cell wall digestibility, on the other hand, is insensitive to N supply (not shown).

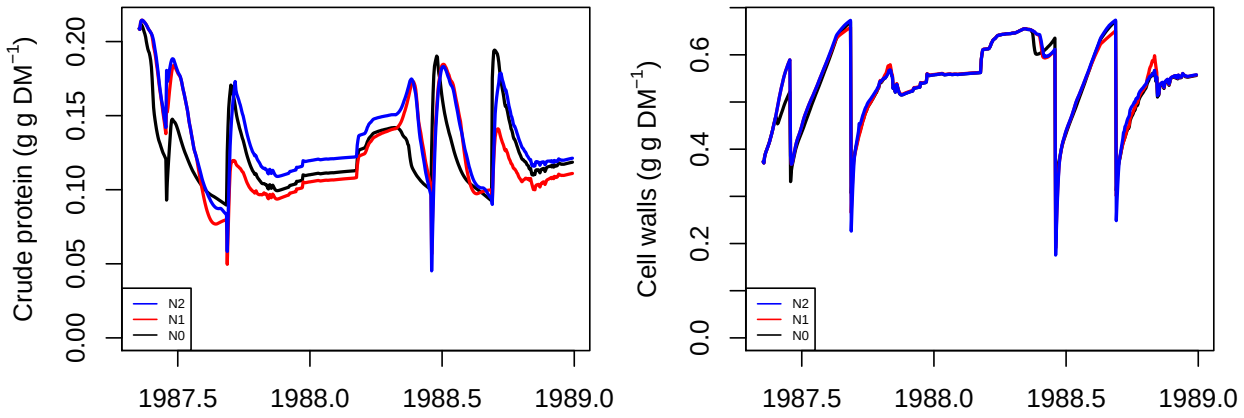

Figure 6: Simulated protein and cell wall concentrations in the biomass, at Kungsängen 1987-1988 for N application rates 0 (NO), 140 (N1), and 200 (N2) kg N ha^{-1} $year^{-1}$

3.2.2 Effects of N-fertilization on N losses to the environment

Effects of N fertilization on N losses in the example of application of BASGRA_N for Kungsängn are shown in Fig. 7. The upper panels show losses of N due to leaching of NO_3 and emission of N_2O and NO, whereas the lower panel show the content of mineral-N in the soil, the amount of fertilizer N applied, and daily precipitation. All three types of losses increase strongly with increased N fertilization, from very low values in the non-N fertilized sward, to more than ten times higher values at the highest N fertilizer level. We also see that N-leaching and N_2O-emissions are peaking early in spring each season, whereas NO-emissions show similarly high peaks early in spring and immediately after the first cut. In both periods, the losses are highest right after the application of N fertilizer when the uptake capacity of the grass is limited due to low biomass resulting from losses in winter or in connection with harvest as observed in experiments (Hansen et al., 2014, Müller and Sherlock (2004)). Total simulated N-emissions are proportional to total N-fertilisation, which is consistent with the emission-factor approach (for N2O) that the IPCC uses (IPCC, 2019). As biomass accumulation accelerates, most of the available mineral-N in the soil is taken up by the sward and losses decline correspondingly. The greater simulated emission rates in 1988 may be explained by slow spring growth in 1988 due to cold weather conditions, ultimately leading to 40 % lower first harvest yield compared with 1989 (see Supplementary data for DM data). The gaseous losses were more closely linked to the content of mineral-N in the soil than to the amount

and seasonal distribution of precipitation under the simulated conditions (Fig. 7). The results are uncertain as it remains to test the model for N losses.

We further use the metric NUE (Nitrogen Use Efficiency) to demonstrate the effect of different fertilization levels on the environment. For the calculation of NUE (Zhang et al., 2015, see below), the main output from grassland, as N in yield (N_{yield}), and the major inputs like fertilizer(N_{fer}), deposition(N_{dep}), manure(N_{man}) and biological fixation(N_{fix}) are used. This metric implicitly includes the N loss in both leaching and denitrification processes and is therefore the most frequently used indicator for optimal fertilization management when considering climate change and water quality (Yu et al., 2014). Given the good prediction accuracy for DM and crude protein (N) in section 3, a good prediction accuracy for NUE can also be expected.

$$NUE = \frac{N_{yield}}{N_{fer} + N_{dep} + N_{man} + N_{fix}}$$

In Fig. 8, we can find that, with annual N fertilization rate less than 50 Kg/ha, NUE values exceed 1.0 as soil mineral N pool is gradually depleted as most of the mineral N is taken up by the grass, and little N source is supplemented to the soil. Although lower environment costs are expected in the short term, such fertilization practice is unsustainable (EU Nitrogen Expert Panel, 2015). On the other hand, the NUE decreases to about 0.59 when increasing annual N fertilization rate up to 160 Kg/ha, which corresponds well with some experimental results from Northern Sweden (Thorvaldsson and Andersson, 1986). Optimal annual N fertilization rate is about 195-225 Kg/ha with NUE reaching 0.65 at the point where the DM yield reaches its maximum level. This is within the desired range of NUE for cropping systems in Europe (EU Nitrogen Expert Panel, 2015). Higher fertilization rate is environmentally harmful as N is no longer the stress factor for grass growth and thus a large quantity of surplus N is released to the atmosphere and water system.

4 Discussion

BASGRA_N is an extension of the BASGRA model. Like its predecessor, BASGRA_N is unique among grassland models in that it takes into account the effect of stressful winter conditions with

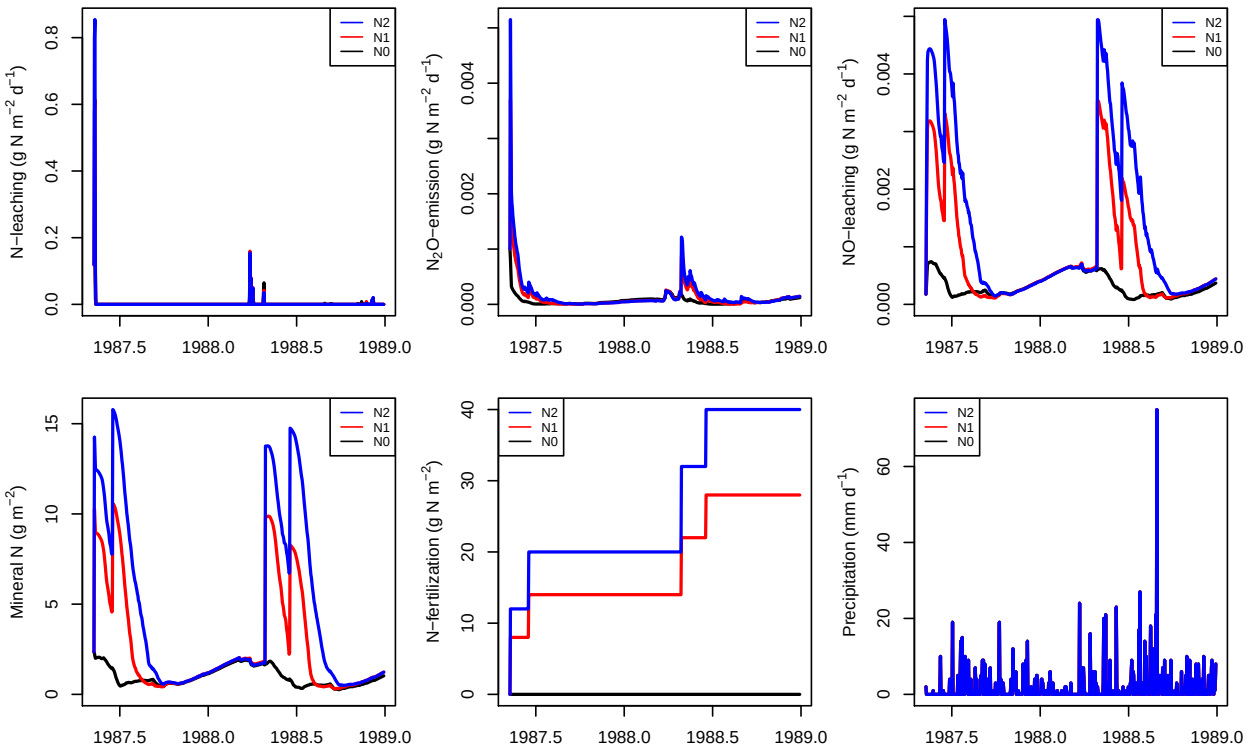

Figure 7: Environmental impacts of N-fertilization at Kungsängen in 1987-1988 for N application rates 0 (NO), 140 (N1), and 200 (N2) kg N ha^{-1} $year^{-1}$

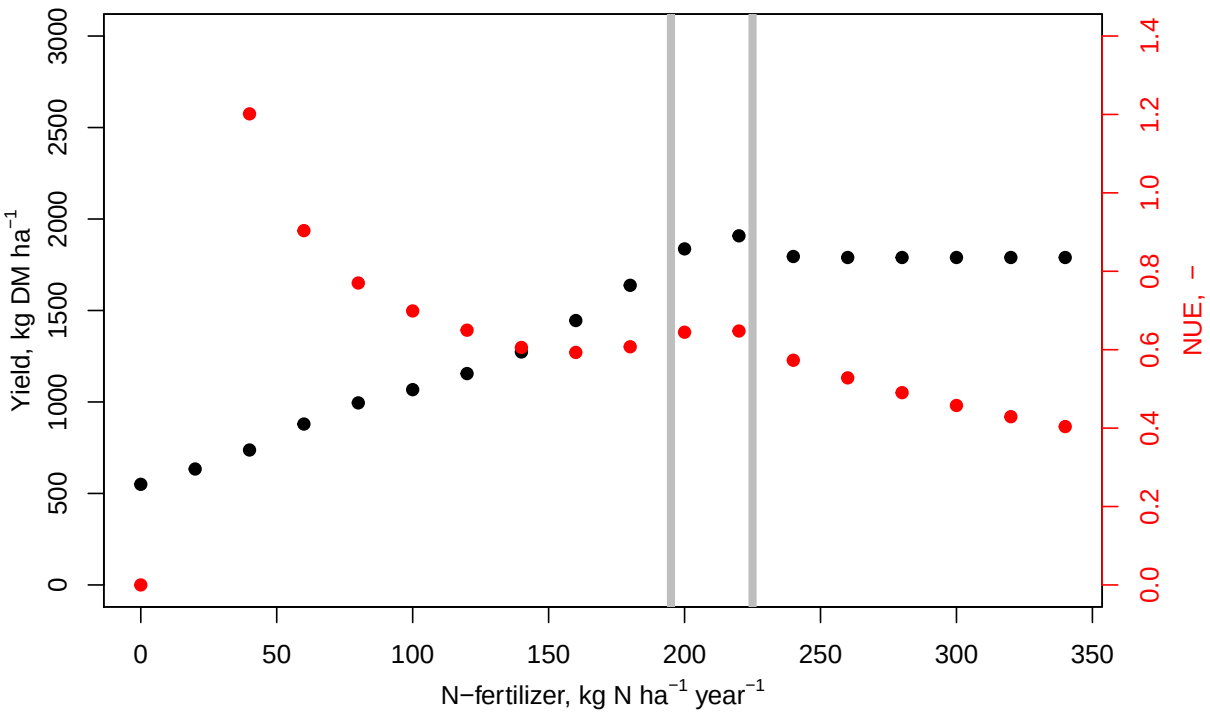

Figure 8: Effect of annual N fertilizer rate on the total accumulated yield and NUE at Kungsängen in 1987-1988. The grey vertical lines indicates the optimal fertilizer range taking into accouunt both productivity criteria and environmental costs

frost, snow and ice exposure on winter survival of tillers, and their subsequent regrowth in spring and seasonal accumulation of harvestable biomass. This is in contrast to other published grassland models that do not account for such winter conditions, although such conditions are common in many regions where timothy is commonly grown, such as in the Scandinavian region for which BASGRA_N was calibrated in the present study. Whereas the older model BASGRA was limited to simulation of mainly the accumulation of harvestable biomass as influenced by genotype, the weather, soil and management factors under non N-limiting conditions, BASGRA_N can also be used to simulate forage nutritive value, C and N cycling and GHG emission, accounting not only for non-N-limiting but also N-limiting conditions. With the present study, we have taken a first step towards such application, by describing the model, calibrating it and evaluating its performance against observations of biomass and nutritive value from field experiments.

4.1 Model behaviour

We carried out two separate calibrations and tests. The Swedish dataset allowed us to compare simulated and observed biomass and CP content under different N fertilizer regimes and a common harvesting regime. The Norwegian dataset allowed us to compare simulated and observed values for 13 different variables including biomass, tiller dynamics of CP, cell wall content (NDF) and DM digestibility as affected by harvesting regime, but under a common N fertilizer regime. The latter dataset was also used to calibrate the previous model BASGRA 2014 (Höglind et al., 2016), allowing for indirect comparison of the performance of BASGRA-N with its predecessor against a common dataset for some key processes and variables.

The simulations for the Swedish test sites indicate good model behaviour for biomass and CP, with overall R^2 larger than 0.58, Willmott's d larger than 0.69 and NRMSE around 0.3 for both variables, and generally well-captured time dynamics. The simulations for the Norwegian site show similarly good results for biomass and CP with good metrics' performance. The comparison of simulated and observed time courses for different N levels indicate that biomass and CP responses to N are well captured in general. However, the graphical results (Fig. S1 and S2) indicate a tendency of less well captured dynamics under severely N-limiting conditions (represented by the non-N fertilized treatment) compared with situations with N fertilization levels corresponding to normal

practice (represented by the N1 and N2 treatments which covers the typical range of variation for N application to Swedish grasslands cut twice yearly).

Although fewer data were available for evaluating the model with respect to simulation of NDF content and digestibility, the results for the Norwegian test site indicate good model behaviour also for these two quality traits, with NRMSE values at least as good as those observed for CP. The time courses for NDF content and digestibility also appear well captured. However, a more thorough evaluation of BASGRA_N is needed with respect to simulation of NDF content and digestibility, including N responses under different growing conditions.

To ensure that the implementation of N response functions does not compromise the ability of BASGRA_N to simulate biomass accumulation and underlying processes, it is of interest to compare the performance of BASGRA_N with its predecessor BASGRA. A comparison of NRMSE for biomass, LAI, reserve content, SLA and tiller density at Særheim in Table 5 with corresponding data for BASGRA (Höglind et al., 2016), indicate that BASGRA_N simulates these processes similarly well as BASGRA, or even slightly better for some of the variables. A strict comparison cannot be made as in the previous study the whole dataset was used for calibration, whereas in the present study it was split into two parts to allow for independent calibration and testing of the model. Nevertheless, the results are promising. The NRMSE values for BASGRA_N presented here are also lower than those observed for a predecessor of BASGRA_N in a model inter-comparison study (0.45 and 0.30 for primary and secondary regrowth, respectively; Korhonen et al. (2018)).

A more thorough evaluation of BASGRA_N with respect to simulation of CP and NDF content and NDF digestibility was recently made in a model inter-comparison study (Persson et al., 2019). The referred study includes observations from a wide range of agro-climatic conditions across the Nordic region and Canada, and comparisons of the performance of BAGRA_N with two other process based models, CATIMO and STICS. The referred study with a larger dataset confirms the conclusions of the present study, indicating good model behaviour, especially for NDF attributes, with NRMSE values of 0.16, 0.09, and 0.08 for CP concentration, NDF concentration, and NDF digestibility, respectively, for the comparison of simulated and observed values in the test dataset for generically calibrated models. The referred study also shows that BASGRA compares well with the other two models with respect to simulation of CP and NDF concentrations, and NDF digestibility.

In BASGRA_N, the N-C ratio of leaves decreases exponentially from the top (Fig. 2). Such an exponential decrease is common in multiple crops including cereals and other Poaceae (Duan et al., 2019; D'Odorico et al., 2019; Li et al., 2013). Vertical N-profiles have recently received renewed research interest because of the need to interpret remote sensing images, which can only see the upper surface of the canopy (Duan et al., 2019; Gara, 2018; Gara et al., 2019; Li et al., 2013; Ye et al., 2018). D'Odorico et al. (2019) showed that including N-profiles improved the accuracy of crop photosynthesis modelling for barley and rape seed.

In the papers by Korhonen et al.(2018) and Persson et al. (2019), BASGRA-N was compared with the well-established models STICS and CATIMO with respect to simulation of timothy growth and N dynamics. As BASGRA-N performed at least as well as the other two models in these respects, we conclude that the N profile approach that was introduce in the present paper works appropriately. In the model comparison study by Korhonen et al (2018), all models performed less well for LAI than for biomass yield, in line with what we observed for BASGRA-N in the present study.

For some model results, we found no comparable information in the literature nor did we have any data. This was the case for tiller dynamics (the fraction of vegetative, non-elongating and elongating generative tillers in swards receiving different levels of N fertilizer, and their winter survival) and fluxes of C and N in the grassland system, including system losses (soil respiration, N_2O-emission. N leaching). Such model results remain speculative until measurements become available.

With this restriction, some general observations could be made for a few variables for which we do not have Scandinavian data, but for which data on N responses in other environments are available in the literature. This includes observations of leaf and tiller dynamics in Canadian timothy swards receiving different amounts of N (Bélanger, 1998; Bélanger and Richards, 1997). The following time course patterns/responses to N were observed both in the Canadian fields and in the simulations for Scandinavian swards in the present study: (1) a positive response of LAI to increasing N supply, with earlier and higher peak LAI values occurring at high compared to moderate N supply, (2) increasing leaf elongation rate (LER) and leaf appearance rate (LAR) with increasing N supply, LER being more sensitive to N supply than LAR, (3) a positive responses of tiller density to increasing N supply, with earlier and higher peak densities occurring at high compared to low N conditions.

N_2O emissions constitutes an important route for N losses from fertilized grasslands to the environment. Evaluation of the model with respect to N_2O emissions require more detailed information than what is currently is available from Scandinavian swards. However, the general behaviour of the model appears reasonably good with simulated N_2O emissions that corresponds well with published data, (Hansen et al., 2014, Müller and Sherlock (2004)) typically showing: highly fluctuating emissions over the season, and distinct emission peaks in connection with and immediately after the application of N fertilizers or N-rich manure. Simulated peak emission values (up to approx. 5 mg N_2O-N m^{-2} d^{-1}; Fig. 7) also correspond well with observed peak values (mg N_2O-N m^{-2} d^{-1}) 3 in a cut sward in Norway receiving 280 kg N ha^{-1} (Hansen et al., 2014), 5 in a cut sward in Germany receiving 200 kg N ha^{-1}, and 12 in a pasture in New Zealand receiving 500 kg N ha^{-1} (Müller and Sherlock, 2004). Further evaluation of the model with respect to N_2O emissions should ideally include continuous data from multi-year experiments including different N fertilizer regimes.

Another important route for N losses from grasslands besides N_2O emission is leaching of NO_3-N. The simulated accumulated annual leaching in the high-N treatment in the example of model application (15 kg N ha^{-1} $year^{-1}$) falls within the observed range of variation for correspondingly fertilized grass on silty sand in Norway in a lysimeter study (10-20 kg N ha^{-1} $year^{-1}$; Korsaeth et al. (2003)) but is slightly higher than the range of variation observed for clay soils in corresponding studies in the Nordic countries (2-7 kg N ha^{-1} $year^{-1}$; Valkama et al. (2016)). However, as for N_2O emissions, further evaluation of BASGRA_N as regards N-leaching should be carried out when suitable data become available.

4.2 Model application

A model like BASGRA_N that takes into account the effect of weather conditions, management and cultivar on plant growth, winter survival, forage yield and quality development, and potential losses of C and N from the forage production system to the environment can be applied in many types of studies, addressing various types of questions. To highlight the applicability of the model, we showed an example in which the model was used to study the effect of N fertilization on the quantity and quality of biomass, and its impact on the environment including greenhouse gas emissions and N budgets for one of the test sites. Beforehand it was expected that high rates of fertilization would

increase both the quantity of growth and greenhouse gas emissions, but might have mixed effects on nutritive value. This was confirmed in the simulation example. Thus, while DM yield and CP increased to large extent with increasing N supply, cell wall content was only slightly affected via indirect effects of fertilizer N on the leaf:stem ratio of biomass. The emission of NO and N_2O also increased with increasing N supply. However, in this simulation example the gaseous losses were small compared to the amount of N taken up by the plants and harvested from the field. Besides, we show an exampled of model application to predict the relationship bewtween N fertilization rate, grass yield and NUE. This type of application provides effective information for both farmers and policy makers to plan their management practices based on different goals. To determine the optimal N fertilizer strategy for any specific location, simulations for longer sequences would be needed to account for the interannual variability in growing conditions, affecting both the timing of management operations, transformation and transport of N in the soil, and plant growth.

4.3 Future work

We have pointed out the need for further testing of the model for the variables for which we currently do not have enough detailed data, notably leaching and emission of N-containing compounds, and tiller dynamics during winter as affected by N supply.

Field experiments for model calibration and testing should ideally include time courses of all the major output variables (typically biomass growth, leaching and emissions as key output variables for calibration and evaluation of underlying processes). However, such experiments are very resource demanding, and therefore rare. Like in the present study, data from different types of experiments will therefore normally be used to evaluate different aspects of a model. Since the two datasets used here represented different cultivars, and cultivar-specific calibration improves prediction accuracy (Korhonen et al., 2018), we did not combine them in the calibration. However, as soon as more data become available, the testing could be repeated and the need for cultivar-specific calibration evaluated against the purpose of the model application.

The previous model version, BASGRA, has mainly been applied to address research questions related to forage production on mineral soils. We are now developing BASGRA_N further by incorporating

functions that will improve its capability to simulate forage grass production, C and N dynamics on organic soils, which are typically characterized by sub-optimal infiltration and drainage conditions, creating prolonged periods of hypoxia and anoxia affecting the biogeochemical cycle (Kløve et al., 2017). For this purpose, experiments are currently being carried out on different locations in Norway to quantify the impact of water table level on grassland productivity and greenhouse gas emissions from organic soils. The experiments will include comprehensive measurements of soil moisture, CO_2, N_2O and CH_4, in addition to quantity and quality of biomass.

Other potential applications of BASGRA_N include identification of ideotypes as basis for plant breeding, as we have shown in a previous study using BASGRA (Van Oijen and Höglind, 2016), and applying it in risk analyses (Van Oijen et al., 2014). The latter showed how climate change could alter risks posed by droughts to C fluxes in grasslands and other vegetation. Future studies could assess risks posed by increased autumn precipitation and less stable winter conditions to C and N fluxes, conditions typically projected for Scandinavia (Rapacz et al., 2014).

BASGRA_N can also be parameterized for other grassland species (Hjelkrem et al., 2017), and work is currently in progress of adapting the model to perennial ryegrass in New Zealand, involving interactions with grazers (J. Woodward, pers. comm.). Work is also in progress on a version of BASGRA for sedge focusing on below-ground processes (A. Dathe, pers. comm).

5 Conclusion and outlook

The main objective of this paper was to present the new model BASGRA_N, to show how it was parameterized for grass swards in Scandinavia, and to evaluate its performance with respect to variables for which sufficient data are available. Special attention was given to the simulation of N responses, as BASGRA_N differs from its predecessor in that it includes N response functions. Based on the results, we conclude that BASGRA_N can be used to simulate yield and CP responses to N with satisfactory precision, while maintaining key features from its predecessor, notably the capability to simulate plant responses to stressful winter conditions typical for high-latitude regions. The results also suggest that content and digestibility of cell walls can be simulated satisfactorily; a conclusion that is further supported by result from a recent model comparison study including data

from a wider range of agro-climatic conditions (Persson et al., 2019). However, further testing of the model is needed for some variables for which we currently do not have enough data, notably leaching and emission of N-containing compounds, and tiller dynamics during winter as affected by N supply. Further work will include adaption of the model with respect to simulation of forage grass yield, C and N dynamics on organic soils, application of the model to investigate GHG mitigation options, and validation against independent data for the conditions for which it will be applied.

6 Acknowledgments

This work was carried out as part of the knowledge-hub Modelling European Agriculture with Climate Change for Food Security (MACSUR) in the Joint Programming Initiative for Agriculture, Climate Change, and Food Security (FACCE-JPI). M.H and T.P. thank the Norwegian Research Council for funding their participation in MACSUR, and Norwegian Institute of Bioeconomy Research (NIBIO) for additional funding. M.v.O. and D.C. thank the Natural Environment Research Council in the U.K. for funding their participation in MACSUR and NIBIO for additional support. We thank Bengt Thorssell and Henrik Eckersten for providing the Swedish dataset in a suitable format for modelling.

7 Appendix A. Supplementary data

Supplementary data associated with this article can be found in the online version.

References

Bélanger, G., 1998. Morphogenetic characteristics of timothy grown with varying N nutrition.

Bélanger, G., Richards, J.E., 1997. Growth analysis of timothy grown with varying N nutrition.

Bonesmo, H., Bélanger, G., 2002. Timothy Yield and Nutritive Value by the CATIMO Model: II.

Digestibility and fiber. Agronomy Journal 94, 345–350. https://doi.org/10.2134/agronj2002.3450

Charles-Edwards, D.A., 1982. Physiological determinants of crop growth. Sydney ; London : Academic Press.

Dreccer, M., Van Oijen, M., Schapendonk, A., Pot, C., Rabbinge, R., 2000. Dynamics of vertical leaf nitrogen distribution in a vegetative wheat canopy. Impact on canopy photosynthesis. Annals of Botany 86, 821–831. https://doi.org/10.1006/anbo.2000.1244

Duan, D., Zhao, C., Li, Z., Yang, G., Zhao, Y., 2019. Estimating total leaf nitrogen concentration in winter wheat by canopy hyperspectral data and nitrogen vertical distribution. Journal of Integrative Agriculture 18, 1562–1570. https://doi.org/10.1016/S2095-3119(19)62686-9

Dumont, B., Andueza, D., Niderkorn, V., Lüscher, A., Porqueddu, C., Picon-Cochard, C., 2015. A meta-analysis of climate change effects on forage quality in grasslands: Specificities of mountain and Mediterranean areas. Grass and Forage Science 70, 239–254. https://doi.org/10.1111/gfs.12169

D'Odorico, P., Emmel, C., Revill, A., Liebisch, F., Eugster, W., Buchmann, N., 2019. Vertical patterns of photosynthesis and related leaf traits in two contrasting agricultural crops. Functional Plant Biology 46, 213–227. https://doi.org/110.1071/FP18061

Eckersten, H., Torssell, B., Kornher, A., Boström, U., 2007. Modelling biomass, water and nitrogen in grass ley: Estimation of N uptake parameters. European Journal of Agronomy 27, 89–101. https://doi.org/10.1016/j.eja.2007.02.003

EU Nitrogen Expert Panel, 2015. Nitrogen Use Efficiency (NUE) - an indicator for the utilization of nitrogen. Wageningen University, Alterra, Wageningen, Netherlands.

Gara, T.W., 2018. Impact of Vertical Canopy Position on Leaf Spectral Properties and Traits across Multiple Species. Remote sensing 10, 346. https://doi.org/10.3390/rs10020346

Gara, T.W., Skidmore, A.K., Darvishzadeh, R., Gara, T.W., Skidmore, A.K., Darvishzadeh, R., 2019. Leaf to canopy upscaling approach affects the estimation of canopy traits. GIScience & Remote Sensing 56, 554–575. https://doi.org/10.1080/15481603.2018.1540170

Goudriaan, J., 1990. Atmospheric CO2, global carbon fluxes and the biosphere, in: Rabbinge, R.,

Goudriaan, J., Van Keulen, H., Penning de Vries, F., Van Laar, H. (Eds.), Theoretical Production Ecology: Reflections and Prospects, Simulation Monographs. Pudoc, Wageningen, pp. 17–40.

Graux, A.I., Bellocchi, G., Lardy, R., Soussana, J.F., 2013. Ensemble modelling of climate change risks and opportunities for managed grasslands in France. Agricultural and Forest Meteorology 170, 114–131. https://doi.org/10.1016/j.agrformet.2012.06.010

Gustavsson, A.-M., Angus, J.F., Torssell, B.W.R., 1995. An Integrated Model for Growth and Nutritional Value of Timothy. Agricultural Systems 1, 73–92.

Hansen, S., Bernard, M.E., Rochette, P., Whalen, J.K., Dorsch, P., 2014. Nitrous oxide emissions from a fertile grassland in Western Norway following the application of inorganic and organic fertilizers. Nutrient Cycling in Agroecosystems 98, 71–85. https://doi.org/DOI 10.1007/s10705-014-9597-x

Hikosaka, K., 2016. Optimality of nitrogen distribution among leaves in plant canopies. Journal of Plant Research 129, 299–311. https://doi.org/10.1007/s10265-016-0824-1

Hjelkrem, A.-G.R., Höglind, M., van Oijen, M., Schellberg, J., Gaiser, T., Ewert, F., 2017. Sensitivity analysis and Bayesian calibration for testing robustness of the BASGRA model in different environments. Ecological Modelling 359, 80–91. https://doi.org/10.1016/j.ecolmodel.2017.05.015

Höglind, M., Hanslin, H., Van Oijen, M., 2005. Timothy regrowth, tillering and leaf area dynamics following spring harvest at two growth stages. Field Crops Research 93, 51–63. https://doi.org/10.1016/j.fcr.2004.09.009

Höglind, M., Schapendonk, A., Van Oijen, M., 2001. Timothy growth in Scandinavia: Combining quantitative information and simulation modelling. New Phytologist 151, 355–367.

Höglind, M., Thorsen, S.M., Semenov, M.a., 2013. Assessing uncertainties in impact of climate change on grass production in Northern Europe using ensembles of global climate models. Agricultural and Forest Meteorology 170, 103–113. https://doi.org/10.1016/j.agrformet.2012.02.010

Höglind, M., Van Oijen, M., Cameron, D., Persson, T., 2016. Process-based simulation of growth and overwintering of grassland using the BASGRA model. Ecological Modelling 335, 1–15. https:

//doi.org/10.1016/j.ecolmodel.2016.04.024

IPCC, 2019. 2019 Refinement to the 2006 IPCC Guidelines for National Greenhouse Gas Inventories. https://www,ipcc.ch/report/2019-refinement-to-the-2006-ipcc-guidelines-for-national-greenhouse-gas-inventories/.

Jégo, G., Bélanger, G., Tremblay, G.F., Jing, Q., Baron, V.S., 2013. Calibration and performance evaluation of the STICS crop model for simulating timothy growth and nutritive value. Field Crops Research 151, 65–77. https://doi.org/10.1016/j.fcr.2013.07.003

Kipling, R.P., Virkajärvi, P., Breitsameter, L., Curnel, Y., De Swaef, T., Gustavsson, A.M., Hennart, S., Höglind, M., Järvenranta, K., Minet, J., Nendel, C., Persson, T., Picon-Cochard, C., Rolinski, S., Sandars, D.L., Scollan, N.D., Sebek, L., Seddaiu, G., Topp, C.F.E., Twardy, S., Van Middelkoop, J., Wu, L., Bellocchi, G., 2016. Key challenges and priorities for modelling European grasslands under climate change. Science of the Total Environment 566-567, 851–864. https://doi.org/10.1016/j.scitotenv.2016.05.144

Kløve, B., Berglund, K., Berglund, Ö., Weldon, S., Maljanen, M., 2017. Future options for cultivated Nordic peat soils: Can land management and rewetting control greenhouse gas emissions? Environmental Science and Policy 69, 85–93. https://doi.org/10.1016/j.envsci.2016.12.017

Korhonen, P., Palosuo, T., Persson, T., Höglind, M., Jégo, G., Van Oijen, M., Gustavsson, A.-M., Bélanger, G., Virkajärvi, P., 2018. Modelling grass yields in northern climates – a comparison of three growth models for timothy. Field Crops Research 224, 37–47. https://doi.org/10.1016/j.fcr.2018.04.014

Korsaeth, A., Bakken, L.R., Riley, H., 2003. Nitrogen dynamics of grass as affected by N input regimes, soil texture and climate - Lysimeter measurements and simulations. Nutrient Cycling in Agroecosystems 66, 181–200. https://doi.org/Doi 10.1023/A:1023928717599

Larsen, A., 1994. Breeding winter hardy grasses. Euphytica 77, 231–237. https://doi.org/doi.org/10.1007/BF02262635

Li, H., Zhao, C., Huang, W., Yang, G., 2013. Field Crops Research Non-uniform vertical nitrogen distribution within plant canopy and its estimation by remote sensing : A review. Field Crops

Research 142, 75–84. https://doi.org/10.1016/j.fcr.2012.11.017

Metropolis, N., Rosenbluth, A., Rosenbluth, M., Teller, A., 1953. Equation of state calculations by fast computing machines. The Journal of Chemical Physics 21, 1087–1095. https://doi.org/org/10.1063/1.1699114

Müller, C., Sherlock, R.R., 2004. Nitrous oxide emissions from temperate grassland ecosystems in the Northern and Southern Hemispheres. Global Biogeochemical Cycles 18, n/a–n/a. https://doi.org/10.1029/2003GB002175

Nordheim-Viken, H., Volden, H., 2009. Effect of maturity stage, nitrogen fertilization and seasonal variation on ruminal degradation characteristics of neutral detergent fibre in timothy (Phleum pratense L.). Animal Feed Science and Technology 149, 30–59. https://doi.org/10.1016/j.anifeedsci.2008.04.015

Persson, T., Höglind, M., 2013. Impact of climate change on harvest security and biomass yield of two timothy ley harvesting systems in Norway. The Journal of Agricultural Science 152, 1–12. https://doi.org/10.1017/S0021859612001013

Persson, T., Höglind, M., Van Oijen, M., Korhonen, P., Palosuo, T., Jégo, G., Virkajärvi, P., Bélanger, G., Gustavsson, A.-M., 2019. Simulation of timothy nutritive value: A comparison of three process-based models. Field Crops Research 231, 81–92. https://doi.org/10.1016/j.fcr.2018.11.008

Rapacz, M., Ergon, Å., Höglind, M., Jørgensen, M., Jurczyk, B., Østrem, L., Arne, O., Marte, A., 2014. Plant Science Overwintering of herbaceous plants in a changing climate . Still more questions than answers. Plant Science 225, 34–44. https://doi.org/10.1016/j.plantsci.2014.05.009

Reynolds, S., Frame, J., 2005. Grasslands: Developments, opportunities, perspectives. CRC Press.

Riedo, M., Grub, A., Rosset, M., Fuhrer, J., 1998. A pasture simulation model for dry matter production, and fluxes of carbon, nitrogen, water and energy. Ecological Modelling 105, 141–183. https://doi.org/10.1016/S0304-3800(97)00110-5

Rodriguez, D., Van Oijen, M., Schapendonk, A., 1999. LINGRA-CC: A sinkSource model to simulate the impact of climate change and management on grassland productivity. New Phytologist

144, 359–368.

Ryan, E.M., Ogle, K., Peltier, D., Walker, A.P., De Kauwe, M.G., Medlyn, B.E., Williams, D.G., Parton, W., Asao, S., Guenet, B., Harper, A.B., Lu, X., Luus, K.A., Zaehle, S., Shu, S., Werner, C., Xia, J., Pendall, E., 2017. Gross primary production responses to warming, elevated CO2, and irrigation: Quantifying the drivers of ecosystem physiology in a semiarid grassland. Global Change Biology 23, 3092–3106. https://doi.org/10.1111/gcb.13602

Thorvaldsson, G., Andersson, S., 1986. Variations in timothy dry matter yield and nutritional value as affected by harvest date, nitrogen fertilization, year and location in Northern Sweden. Acta Agriculturae Scaninavica 36, 367–385. https://doi.org/10.1080/00015128609439895

Valkama, E., Rankinen, K., Virkajärvi, P., Salo, T., Kapuinen, P., Turtola, E., 2016. Nitrogen fertilization of grass leys: Yield production and risk of N leaching. Agriculture, Ecosystems and Environment 230, 341–352. https://doi.org/10.1016/j.agee.2016.05.022

Van Oijen, M., Balkovi, J., Beer, C., Cameron, D.R., Ciais, P., Cramer, W., Kato, T., Kuhnert, M., Martin, R., Myneni, R., Rammig, A., Rolinski, S., Soussana, J.F., Thonicke, K., Van Der Velde, M., Xu, L., 2014. Impact of droughts on the carbon cycle in European vegetation: A probabilistic risk analysis using six vegetation models. Biogeosciences 11, 6357–6375. https://doi.org/10.5194/bg-11-6357-2014

Van Oijen, M., Bellocchi, G., Höglind, M., 2018. Effects of Climate Change on Grassland Biodiversity and Productivity: The Need for a Diversity of Models. Agronomy 8, 14. https://doi.org/10.3390/agronomy8020014

Van Oijen, M., Dreccer, M., Firsching, K.-H., Schnieders, B., 2004. Simple equations for dynamic models of the effects of CO2 and O3 on light-use efficiency and growth of crops. Ecological Modelling 179, 39–60. https://doi.org/10.1016/j.ecolmodel.2004.05.002

Van Oijen, M., Höglind, M., 2016. Toward a Bayesian procedure for using process-based models in plant breeding, with application to ideotype design. Euphytica 207, 627–643. https://doi.org/10.1007/s10681-015-1562-5

Van Oijen, M., Höglind, M., Hanslin, H.M., Caldwell, N., 2005. Process-Based Modeling of Timothy

Regrowth. Agronomy Journal 97, 1295. https://doi.org/10.2134/agronj2004.0251

Van Oijen, M., Rougier, J., Smith, R., 2005. Bayesian calibration of process-based forest models: Bridging the gap between models and data. Tree Physiology 25, 915–927.

Wu, L., McGechan, M.B., McRoberts, N., Baddeley, J.A., Watson, C.A., 2007. SPACSYS: Integration of a 3D root architecture component to carbon, nitrogen and water cycling description. Ecological Modelling 200, 343–359. https://doi.org/10.1016/j.ecolmodel.2006.08.010

Wu, L., Rees, R., Tarsitano, D., Zhang, X., Jones, S., Whitmore, A., 2015. Simulation of nitrous oxide emissions at field scale using the SPACSYS model. The Science of the Total Environment 530-531, 76–86. https://doi.org/10.1016/j.scitotenv.2015.05.064

Ye, H., Huang, W., Huang, S., Wu, B., Dong, Y., 2018. Remote Estimation of Nitrogen Vertical Distribution by Consideration of Maize Geometry Characteristics. Remote sensing 10, 1995. https://doi.org/10.3390/rs10121995

Yu, C., Huang, X., Chen, H., Godfray, H.C.J., Wright, J.S., Jim, W., Gong, P., Ni, S., Qiao, S., Huang, G., Xiao, Y., Zhang, J., Feng, Z., Ju, X., Ciais, P., Stenseth, N.C., 2014. Managing nitrogen to restore water quality in China. Nature 567, 516–520. https://doi.org/10.1038/s41586-019-1001-1

Zhang, X., Davidson, E.A., Mauzerall, D.L., Searchinger, T.D., Dumas, P., Shen, Y., 2015. Managing nitrogen for sustainable development. Nature 528, 51–59. https://doi.org/10.1038/nature15743